

Association of TDP-43 Pathology with Global and Regional ^{18}F -Florbetapir PET Signal in the Alzheimer's Disease Spectrum

Stefan J. Teipel^{a,b,*}, Anna Gesine Marie Temp^a, Fedor Levin^a,
Martin Dyrba^a and Michel J. Grothe^{a,c,*} for the Alzheimer's Disease Neuroimaging Initiative¹
^aGerman Center for Neurodegenerative Diseases (DZNE), Rostock, Germany
^bDepartment of Psychosomatic Medicine, University Medicine Rostock, Rostock, Germany
^cUnidad de Trastornos del Movimiento, Servicio de Neurología y Neurofisiología Clínica, Instituto de Biomedicina de Sevilla, Hospital Universitario Virgen del Rocío/CSIC/Universidad de Sevilla, Seville, Spain

Accepted 30 October 2020
Pre-press 13 December 2020

Abstract.

Background: TAR DNA-binding protein 43 (TDP-43) has been recognized as a frequent co-pathology of Alzheimer's disease (AD). The effect of the presence of TDP-43 pathology on *in vivo* measures of AD-related amyloid pathology using amyloid sensitive PET is still unresolved.

Objective: To study the association of TDP-43 pathology with antemortem amyloid PET signal.

Methods: We studied 30 cases from the ADNI autopsy sample with available ratings of presence of TDP-43 and antemortem amyloid sensitive ^{18}F -FlorbetapirPET. We used Bayesian regression to determine the effect of TDP-43 on global and regional amyloid PET signal. In a *post-hoc* analysis, we assessed the association of TDP-43 pathology with antemortem memory performance.

Results: We found substantial to strong evidence for a negative effect of TDP-43 (Bayes factor against the null model (BF_{10}) = 9.0) and hippocampal sclerosis (BF_{10} = 6.4) on partial volume corrected hippocampal ^{18}F -Florbetapir uptake. This effect was only partly mediated by the negative effect of TDP-43 on hippocampal volume. In contrast, Bayesian regression supported that there is no effect of TDP-43 on global cortical PET-signal (BF_{10} = 0.65). We found an anecdotal level of evidence for a negative effect of TDP-43 pathology on antemortem memory performance after accounting for global amyloid PET signal (BF_{10} = 1.6).

Conclusion: Presence of TDP-43 pathology does not confound the global amyloid PET-signal but has a selective effect on hippocampal PET-signal that appears only partially dependent on TDP-43 mediated atrophy.

Keywords: Amyloid pathology, florbetapir PET, hippocampal sclerosis, hippocampal volume, memory, TAR DNA-binding protein 43

¹Data used in preparation of this article were obtained from the Alzheimer's Disease Neuroimaging Initiative (ADNI) database (<http://adni.loni.usc.edu/>). As such, the investigators within the ADNI contributed to the design and implementation of ADNI and/or provided data but did not participate in analysis or writing of this report. A complete listing of ADNI investigators can be found at: http://adni.loni.usc.edu/wp-content/uploads/how_to_apply/ADNI_Acknowledgement_List.pdf

*Correspondence to: Stefan J. Teipel, MD, Department of Psychosomatic Medicine, University Medicine Rostock, and DZNE Rostock, Gehlsheimer Str. 20, 18147 Rostock, Germany. Tel.: +01 149 381 494 9470; Fax: +01149 381 494 9682; E-mail: stefan.teipel@med.uni-rostock.de. and Michel J. Grothe, PhD, Unidad de Trastornos del Movimiento, Instituto de Biomedicina de Sevilla (IBiS), Avda. Manuel Siurot s/n, 41013 Seville, Spain. Tel.: +34 955 923 000; Fax: +34 955 923 101; E-mail: neurosev@gmail.com.

INTRODUCTION

Clinico-pathological association studies have established that global increase of amyloid sensitive positron emission tomography (PET) signal reflects the cerebral accumulation of amyloid- β (A β) pathology [1–4]. Additionally, comorbid non-Alzheimer's disease (AD) pathology may impact the amyloid PET signal [5]. One frequent comorbid pathology of AD is the presence of the TAR DNA-binding protein 43 (TDP-43) with and without hippocampal sclerosis [6].

Here, we used ^{18}F -Florbetapir-PET scans and neuropathological data from the Alzheimer's Disease Neuroimaging Initiative (ADNI) cohort to determine associations of TDP-43 with and without hippocampal sclerosis with hippocampal ^{18}F -Florbetapir-PET signal. We assessed whether TDP-43 pathology with and without hippocampal sclerosis would be inversely associated with ^{18}F -Florbetapir-PET signal in the hippocampus, reflecting the degree of TDP-43 related hippocampus atrophy [7]. In addition, we assessed the contribution of TDP-43 pathology to global amyloid PET signal.

MATERIAL AND METHODS

Data source

Data used in the preparation of this article were obtained from the ADNI database (<http://adni.loni.usc.edu/>). The ADNI was launched in 2003 by the National Institute on Aging, the National Institute of Biomedical Imaging and Bioengineering, the Food and Drug Administration, private pharmaceutical companies and non-profit organizations, with the primary goal of testing whether neuroimaging, neuropsychologic, and other biologic measurements can be used as reliable *in vivo* markers of AD pathogenesis. A fuller description of ADNI and up-to-date information is available at <http://www.adni-info.org>.

Standard protocol approvals, registrations, and patient consents

All procedures performed in the ADNI studies involving human participants were in accordance with the ethical standards of the institutional research committees and with the 1964 Helsinki declaration and its later amendments. Written informed consent was obtained from all participants and/or authorized

representatives and the study partners before any protocol-specific procedures were carried out in the ADNI studies.

Study participants

We retrieved the last available ^{18}F -Florbetapir-PET scans of 30 ADNI subjects who had come to autopsy between 2007 and 2017. Detailed inclusion criteria for the antemortem diagnostic categories can be found at the ADNI web site (<http://adni.loni.usc.edu/methods/>). Cognitively normal (CN) subjects had MMSE scores between 24–30 (inclusive), a CDR=0, were non-depressed, non-mild cognitive impairment (MCI), and non-demented, and reported no subjective memory concerns. MCI subjects had Mini-Mental State Examination (MMSE) scores between 24–30 (inclusive), a subjective memory concern reported by subject, informant, or clinician, objective memory loss measured by education adjusted scores on delayed recall, a Clinical Dementia Rating (CDR)=0.5, absence of significant levels of impairment in other cognitive domains, essentially preserved activities of daily living, and an absence of dementia. At inclusion into the ADNI cohort subjects with AD dementia had initial MMSE scores between 20–26 (inclusive), a CDR = 0.5 or 1.0 with impaired activities of daily living, and fulfilled NINCDS-ADRDA criteria for clinically probable AD [8].

Neuropsychological assessment

For association with the presence of TDP-43 we used the last available ADNI composite scores for episodic memory [9].

Neuropathological assessments

All neuropathological evaluations in the ADNI cohort are performed through the central laboratory of the ADNI neuropathology core (<http://adni.loni.usc.edu/about/#core-container>) [10]. The neuropathological procedures follow previously established guidelines [11] that are captured in the format of the Neuropathology Data Form Version 10 of the National Alzheimer Coordinating Center (<https://www.alz.washington.edu/NONMEMBER/NP/npform10.pdf>).

Here, we applied established rating scales for the presence of TDP-43 pathology and hippocampal sclerosis. Presence of TDP-43 pathology was classified

as positive if it was detected in any of the following brain regions: amygdala, hippocampus, and entorhinal cortex/inferior temporal gyrus. In addition, we used regional neuropathological rating scores of diffuse, core, and neuritic plaques within the hippocampal dentate gyrus and CA1 region.

Imaging data acquisition

Detailed acquisition and standardized pre-processing steps of ADNI imaging data are available at the ADNI website (<https://adni.loni.usc.edu/methods/>). Amyloid-PET data was collected during a 50- to 70 min interval following a 370 MBq bolus injection of ^{18}F -Florbetapir. To account for the multicentric acquisition of the data across different scanners and sites, all PET scans undergo standardized pre-processing steps within ADNI.

For anatomical reference and pre-processing of the PET scans we used the corresponding structural magnetic resonance imaging (MRI) scan that was closest in time to the Florbetapir PET scan. MRI data were acquired on multiple 3T MRI scanners using scanner-specific T1-weighted sagittal 3D MPRAGE sequences. Similar to the PET data, MRI scans undergo standardized preprocessing steps aimed at increasing data uniformity across the multicenter scanner platforms (see <https://adni.loni.usc.edu/methods/> for detailed information on multicentric MRI acquisition and preprocessing in ADNI).

Imaging data pre-processing

Images were preprocessed using Statistical Parametric Mapping software version 12 (SPM12) (The Wellcome Trust Centre for Neuroimaging, Institute of Neurology, University College London) implemented in Matlab 2019. MRI images were segmented into different tissue types and spatially normalized to a customized aging/AD-specific reference template [12] using the CAT12 toolbox. The pre-processing pipeline for the amyloid PET images followed the routine previously described in [13]. Partial volume effects (PVE) were corrected in native space using the 3-compartmental voxel-based post-reconstruction method as described by Müller-Gärtner and colleagues [14, 15]. The corrected PET images were spatially normalized to an aging/AD-specific reference template using the deformation parameters derived from the normalization of their corresponding MRI.

PVE-corrected ^{18}F -Florbetapir-PET mean uptake values were calculated for the hippocampus as defined by the Harvard–Oxford structural atlas [16] (<https://fsl.fmrib.ox.ac.uk/fsl/fslwiki/Atlases>), and a global cortical composite mask including frontal, parietal and temporal areas [17]. Hippocampal and global cortical standardized uptake value ratios (SUVR) were obtained by scaling to the mean uptake of the whole cerebellum (in non-corrected ^{18}F -Florbetapir-PET).

Hippocampus volume was derived from the spatially normalized MRI scans using the Harvard–Oxford hippocampal mask and scaled to each individual’s total intracranial volume.

Statistics

We used *Bayes factor (BF) hypothesis testing* to compare one or more alternative hypotheses against the null hypothesis (i.e., the assumption that there is no effect of neuropathological markers, H_0) [18, 19], as implemented in *Jeffreys’ Amazing Statistics Program* (JASP Version 0.11.1), available at <http://jasp-stats.org>. This facilitates the simultaneous comparison of four hypotheses: the absence of an effect (null hypothesis), the effect of TDP-43 alone, the effect of hippocampal sclerosis alone, the combined effect of hippocampal sclerosis and TDP-43. Subsequently, we can determine the hypothesis best supported by our data. We report the Bayes Factor (BF_{10}) quantifying evidence against the null hypotheses, as well as the BF_M indicating the informativeness of our data given the prior ($P(M)$) and posterior distributions ($P(M|\text{data})$) [19]. In addition we report estimates of regression coefficients with corresponding 95% credibility intervals [20]. Bayes factor hypothesis testing inferences are mutually consistent with every single participant’s data contribution through continuous updating of the prior distribution [19] (Fig. 2). Table 1 provides a short description of the Bayesian parameters that are reported here and the applied evidence categories.

We determined associations of presence of TDP-43 pathology and hippocampal sclerosis with global and hippocampal partial volume correction (PVC) SUVR values, including age, sex, and distance between PET scanning and death into the null model. We determined if associations of TDP-43 with hippocampal SUVR were mediated by the effects of TDP-43 on hippocampal volume using Bayesian mediation regression with the packages “brms” and “mediation” in R-Studio, version 1.1.463.

For comparison, we determined associations of dentate gyrus and CA1 region scores for diffuse plaques, core plaques and neuritic plaques with hippocampal PVC SUVR values, including age, sex, and distance between PET scanning and death into the null model.

After supporting the effect of TDP-43 on hippocampal PVC SUVR, but not on global SUVR values, we added a *post hoc* analysis to determine if the presence of TDP-43 was associated with ADNI memory scores controlling for age, sex, distance between testing and death, and global SUVR values.

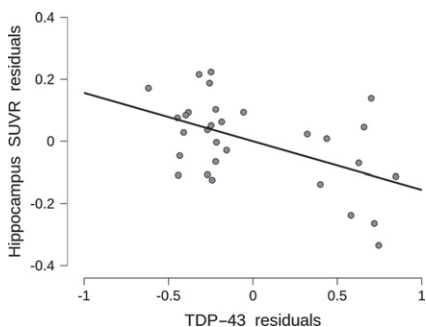


Fig. 1. Association of TDP-43 pathology with antemortem hippocampus SUVR. Hippocampus SUVR residuals are plotted by TDP-43 pathology residuals, after regressing out age, sex, and distance between cognitive testing and death from both variables. The scatter plot includes the least square regression line.

RESULTS

Demographics

Demographics of the sample of 30 cases with available ¹⁸F-Florbetapir-PET scans are given in Table 2. Ten of the thirty cases had indication of TDP-43 pathology; two of these ten cases had hippocampal sclerosis. Global SUVR values ranged between 1.15 and 4.73, i.e., all cases were above a previous used cut-off of 1.04 used for global amyloid positivity in the ADNI autopsy data [21]. In contrast, hippocampal SUVR values ranged between 0.45 and 1.01, with all cases below the previously defined cut-off.

TDP-43, hippocampal sclerosis, hippocampal Aβ pathology, and hippocampal ¹⁸F-Florbetapir SUVR

We found substantial to strong evidence for TDP-43 to be associated with bilateral hippocampal PVC SUVR values (BF₁₀=9.0) when age, sex, and distance between PET and death were included into the null model. The corresponding coefficient for TDP-43 was -0.010 (95-CI: -0.185 to 0). Figure 1 shows a corresponding scatterplot for the TDP-43 effect, and Fig. 2 a sequential robustness check. Adding hippocampal sclerosis to the model showed additional substantial evidence for hippocampal sclerosis alone (BF₁₀=6.4) and very strong evidence for the com-

Table 1
Summary of the reported Bayesian Statistics

Abbreviation	Full Name	Interpretation
BF	Bayes Factor	Quantifies evidence
BF ₁₀	BF in favor of the best model	Data are BF ₁₀ times more likely under the best H ₁ compared to H ₀
BF _M	Degree to which the data have changed the prior model odds	The larger, the more informative the data have been
P(M)	Prior (distribution)	Assumed distribution prior to data analysis
P(M data)	Posterior (distribution)	Distribution after the prior has been updated with the data
95%-CI	Credibility interval	Parameter lies within the lower and upper bounds with 95% probability.
Evidence categories	BF ₁₀ > 3	substantial evidence
	BF ₁₀ > 10	strong evidence
	BF ₁₀ > 30	very strong evidence
	BF ₁₀ > 100	extreme evidence
	BF ₁₀ < 1/3	support for null model

Table 2
Sample characteristics at time of last ¹⁸F-Florbetapir PET scan

N (Controls/MCI/AD)	N (f/m)	Mean age (SD), range [y]	MMSE (SD)	Education [y] (SD)	Average time between Amyloid-PET and death (SD), range [y]
5/3/22	8/22	82.8 (7.6), 59 – 95	20.8 (6.2)	16.6 (2.6)	2.3 (1.3), 0.3 – 5.0

f/m, female/male; SD, standard deviation.

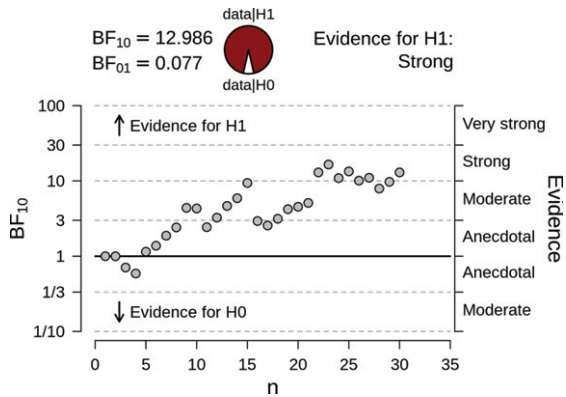


Fig. 2. Sequential robustness check for the effect of TDP-43 on hippocampus SUVR. The probability wheel on top contrasts the posterior probabilities for the data under the assumption of presence (H1) or absence (H0) of an effect of TDP-43. The scatter plot on the bottom demonstrates the internal coherence of Bayesian hypothesis testing: each individual participant contributes to the updating of the prior distribution, and the subsequent inference based on the posterior distribution (shown on the right-hand y-axis). To illustrate this, note participant 14, 15, and 16. Participant 14's data contribution to the summed up inferences from participants 1–13 shifts the BF to just below 10, so in the “moderate” evidence category. The addition of participant 15's data pushes the currently possible conclusion over into the “strong” evidence category. However, when we update the information from participants 1–15 with the data contributed by participant 16, our evidence strength plummets to just above 3. This is what is meant by Bayesian coherence: the conclusions are coherent with every individual participant's contribution and are therefore not limited in their validity by the small sample size. After the inclusion of 20 cases the strong evidence level for the presence of an effect remains stable.

bined effect of TDP-43 and hippocampal sclerosis ($BF_{10} = 18.5$) (Table 3a). When hippocampal sclerosis already was included into the null model, then the data became 2.5 times more likely when adding TDP-43 to it. In the Bayesian mediation analysis, only 32.4% (95-CI: 13.7 – 78.5) of the effect of TDP-43 on hippocampal PVC SUVR was mediated by the effect of TDP-43 on hippocampus volume (Table 3b). The estimates of the coefficients were negative for TDP-43 on hippocampus volume and hippocampal PVC SUVR, and positive for hippocampus volume on hippocampal PVC SUVR.

Evidence was in favor of no effect of TDP-43 on global PVC SUVR values ($BF_{10} = 0.65$). Evidence was in favor of no association of core or diffuse plaque or neuritic plaque scores in the dentate gyrus and the CA1 region with bilateral hippocampal SUVR ($BF_{10} < 0.67$ for all comparisons, in favor of the null model).

We found a negative association between memory score and TDP-43, i.e., lower memory performance with the presence of TDP-43, with a Kendall's tau correlation coefficient of -0.26 (95% credibility interval between -0.47 and 0) (Fig. 3). The Bayes factor, however, indicated only anecdotal evidence in favor of an effect of TDP-43 on the ADNI memory score ($BF_{10} = 1.6$).

DISCUSSION

We found no association of TDP-43 with global PVC SUVR values, consistent with a previous study

Table 3a
Hippocampus SUVR versus TDP-43

TDP-43 main effects					
Models	P(M)	P(M data)	BF_M	BF_{10}	R^2
Null model (incl. age, sex, PET to death)	0.333	0.037	0.076	1.000	0.040
TDP-43 & hippocampal sclerosis	0.333	0.679	4.240	18.486	0.397
TDP-43	0.167	0.166	0.992	9.010	0.295
hippocampal sclerosis	0.167	0.118	0.670	6.431	0.269

Table 3b

Mediation of TDP-43 effect on hippocampal SUVR by hippocampus volume		
(i) Model definition		
Independent predictor: TDP-43		
Mediator: bilateral hippocampus volume		
Dependent variable: hippocampal SUVR		
(ii) Parameter estimates		
	Mean	95-CI
Direct effect: TDP-43 ->hippocampal SUVR	-0.10	[-0.20 0.00]
Indirect effect:	-0.05	[-0.12 0.00]
• TDP-43 ->hippocampus volume	-0.21	[-0.39 -0.03]
• hippocampus volume ->hippocampal SUVR	0.25	[0.05 0.46]
Total effect	-0.15	[-0.25 -0.05]

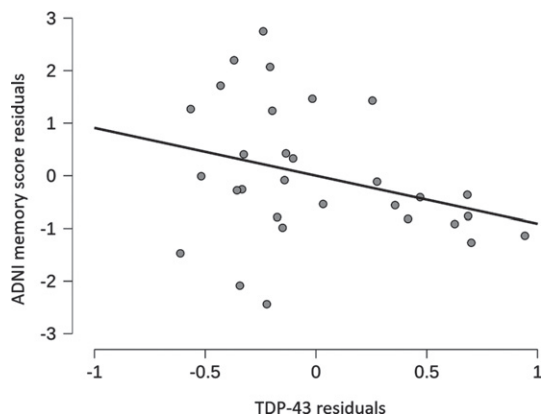


Fig. 3. Association of TDP-43 pathology with antemortem memory performance. ADNI memory score residuals are plotted by TDP-43 pathology residuals, after regressing out age, sex, distance between cognitive testing and death, and global SUVR values from both variables. The scatter plot includes the least square regression line.

[5], but could confirm our assumption that the presence of TDP-43 pathology would be associated with lower levels of hippocampal amyloid PET signal. One major contributor was the presence of hippocampal sclerosis that accounted for some of the TDP-43 effect; however, TDP-43 remained a relevant predictor even when accounting for hippocampal sclerosis. Interestingly, against our expectation, the effect of TDP-43 on hippocampus amyloid PET signal was only partly mediated by the well-known effect of TDP-43 on hippocampus volume [7], with the mediated effect accounting only for about a third of the total effect. Our findings extend results of two previous studies. One study reported in six cases that a negative ^{11}C -PIB-PET scan was associated with different non-AD pathologies, including TDP-43 in two cases [22]. Our findings also agree with observations in 16 amnesic MCI cases with slowly progressive cognitive decline suggestive of limbic TDP-43 pathology/hippocampal sclerosis that showed prominent ^{18}F -FDG-PET hypometabolism in bilateral hippocampus with no to little uptake of ^{18}F -Florbetaben amyloid tracer in the hippocampus [23]. These previous studies suggest that non-AD pathology, including TDP-43, can induce an amnesic clinical phenotype resembling AD in absence of a global and hippocampal increase of amyloid PET signal. The association of hippocampal sclerosis with lower levels of hippocampal amyloid PET signal agrees with a clinico-pathological comparison study in 57 cases [24]. In this study, 13 cases were rated as amyloid negative upon autopsy examination,

with two of these cases featuring both prominent hippocampal sclerosis and negative ^{18}F -Florbetapen-PET scans. Despite these previous findings, the nature of the direct effect of TDP-43 on hippocampal PVC SUVR remains unresolved. One could assume that in the presence of TDP-43 pathology, less amyloid signal in the hippocampus is necessary for a person to be clinically classified into the AD spectrum; however, increased hippocampus amyloid PET signal occurs only late in the course of AD and therefore is not a major driver for diagnostic classification. The finding on TDP-43 and episodic memory performance from the last available assessment of the ADNI memory score would be compatible with the notion that the presence of TDP-43 is associated with the degree of memory dysfunction when controlling for the level of overall amyloid, i.e., in the presence of TDP-43 it takes less amyloid to reach a similar degree of cognitive impairment. However, this evidence was weak as assessed by the Bayes factor and therefore needs to be confirmed in subsequent studies. In the mediation analysis, higher hippocampus volume was associated with a higher amyloid signal in the hippocampus. This finding indicates that even when using a three compartmental correction for partial volume effects [14, 15] the ^{18}F -Florbetapir-PET signal in the highly convoluted area of the hippocampus with close proximity of white matter, grey matter, and cerebrospinal fluid spaces, was partly driven by the amount of remaining grey matter. Our results agree with findings of a previous study in 104 cognitively normal people where hippocampal ^{11}C -PiB retention values without PVC correlated positively with the volume of the left hippocampus derived from MRI [25].

Our findings are limited by the small number of cases. Our data serve to generate rather than confirm the hypothesis that TDP-43 pathology may be associated with hippocampus SUVR in the AD spectrum and require replication in independent cohorts. Such independent replication efforts could apply our posterior distributions (Table 3a) as their prior distributions, testing our newly-generated hypothesis directly. One should note that our findings relate only to ^{18}F -Florbetapir, as other tracers with other binding properties may yield different results. Taking further confounds into account such as non-AD comorbidities beyond TDP-43, such as Lewy body pathology, would have strengthened our results; however, the small number of cases prohibited further stratification of the sample.

In summary, we found that TDP-43 pathology with and without hippocampal sclerosis was associated with lower levels of hippocampus amyloid PET signal beyond its effect on hippocampal atrophy. The underlying nature of this effect remains unclear, as the hippocampal amyloid PET signal itself was more strongly related to the remaining amount of grey matter in this region than to the local degree of A β pathology.

ACKNOWLEDGMENTS

MJG is supported by the “Miguel Servet” program [CP19/00031] of the Spanish Instituto de Salud Carlos III (ISCIII-FEDER).

Data collection and sharing for this project was funded by the Alzheimer’s Disease Neuroimaging Initiative (ADNI) (National Institutes of Health Grant U01 AG024904) and DOD ADNI (Department of Defense award number W81XWH-12-2-0012). ADNI is funded by the National Institute on Aging, the National Institute of Biomedical Imaging and Bioengineering, and through generous contributions from the following: Alzheimer’s Association; Alzheimer’s Drug Discovery Foundation; Araclon Biotech; BioClinica, Inc.; Biogen Idec Inc.; Bristol-Myers Squibb Company; Eisai Inc.; Elan Pharmaceuticals, Inc.; Eli Lilly and Company; EuroImmun; F. Hoffmann-La Roche Ltd and its affiliated company Genentech, Inc.; Fujirebio; GE Healthcare; IXICO Ltd.; Janssen Alzheimer Immunotherapy Research & Development, LLC.; Johnson & Johnson Pharmaceutical Research & Development LLC.; Medpace, Inc.; Merck & Co., Inc.; Meso Scale Diagnostics, LLC.; NeuroRx Research; Neurotrack Technologies; Novartis Pharmaceuticals Corporation; Pfizer Inc.; Piramal Imaging; Servier; Synarc Inc.; and Takeda Pharmaceutical Company. The Canadian Institutes of Health Research is providing funds to support ADNI clinical sites in Canada. Private sector contributions are facilitated by the Foundation for the National Institutes of Health (<http://www.fnih.org>). The grantee organization is the Northern California Institute for Research and Education, and the study is coordinated by the Alzheimer’s Disease Cooperative Study at the University of California, San Diego. ADNI data are disseminated by the Laboratory for Neuro Imaging at the University of Southern California.

Authors’ disclosures available online (<https://www.j-alz.com/manuscript-disclosures/20-1032r1>).

AVAILABILITY OF DATA AND MATERIAL

Data used for the current analysis from the ADNI cohort are freely available from the ADNI website (<http://adni.loni.usc.edu/data-samples/access-data>), including autopsy data and amyloid PET scans. Processed partial volume corrected PET scans are available upon request through the corresponding author of this manuscript.

REFERENCES

- [1] Villeneuve S, Rabinovici GD, Cohn-Sheehy BI, Madison C, Ayakta N, Ghosh PM, La Joie R, Arthur-Bentil SK, Vogel JW, Marks SM, Lehmann M, Rosen HJ, Reed B, Olichney J, Boxer AL, Miller BL, Borys E, Jin LW, Huang EJ, Grinberg LT, DeCarli C, Seeley WW, Jagust W (2015) Existing Pittsburgh Compound-B positron emission tomography thresholds are too high: Statistical and pathological evaluation. *Brain* **138**, 2020-2033.
- [2] Sabri O, Sabbagh MN, Seiby J, Barthel H, Akatsu H, Ouchi Y, Senda K, Murayama S, Ishii K, Takao M, Beach TG, Rowe CC, Leverenz JB, Ghetti B, Ironside JW, Catafau AM, Stephens AW, Mueller A, Koglin N, Hoffmann A, Roth K, Reininger C, Schulz-Schaeffer WJ, Florbetaben Phase 3 Study Group (2015) Florbetaben PET imaging to detect amyloid beta plaques in Alzheimer’s disease: Phase 3 study. *Alzheimers Dement* **11**, 964-974.
- [3] Salloway S, Gamez JE, Singh U, Sadowsky CH, Villena T, Sabbagh MN, Beach TG, Duara R, Fleisher AS, Frey KA, Walker Z, Hunjan A, Escovar YM, Agronin ME, Ross J, Bozoki A, Akinola M, Shi J, Vandenberghe R, Ikonovic MD, Sherwin PF, Farrar G, Smith APL, Buckley CJ, Thal DR, Zanette M, Curtis C (2017) Performance of [(18)F]flutemetamol amyloid imaging against the neuritic plaque component of CERAD and the current (2012) NIA-AA recommendations for the neuropathologic diagnosis of Alzheimer’s disease. *Alzheimers Dement (Amst)* **9**, 25-34.
- [4] Clark CM, Pontecorvo MJ, Beach TG, Bedell BJ, Coleman RE, Doraiswamy PM, Fleisher AS, Reiman EM, Sabbagh MN, Sadowsky CH, Schneider JA, Arora A, Carpenter AP, Flitter ML, Joshi AD, Krautkramer MJ, Lu M, Mintun MA, Skovronsky DM, AV-45-A16 Study Group (2012) Cerebral PET with florbetapir compared with neuropathology at autopsy for detection of neuritic amyloid-beta plaques: A prospective cohort study. *Lancet Neurol* **11**, 669-678.
- [5] Dugger BN, Clark CM, Serrano G, Mariner M, Bedell BJ, Coleman RE, Doraiswamy PM, Lu M, Fleisher AS, Reiman EM, Sabbagh MN, Sadowsky CH, Schneider JA, Zehntner SP, Carpenter AP, Joshi AD, Mintun MA, Pontecorvo MJ, Skovronsky DM, Sue LI, Beach TG (2014) Neuropathologic heterogeneity does not impair florbetapir-positron emission tomography postmortem correlates. *J Neuropathol Exp Neurol* **73**, 72-80.
- [6] Wilson AC, Dugger BN, Dickson DW, Wang DS (2011) TDP-43 in aging and Alzheimer’s disease - a review. *Int J Clin Exp Pathol* **4**, 147-155.
- [7] Josephs KA, Whitwell JL, Knopman DS, Hu WT, Stroh DA, Baker M, Rademakers R, Boeve BF, Parisi JE, Smith GE, Ivnik RJ, Petersen RC, Jack CR, Jr., Dickson DW (2008) Abnormal TDP-43 immunoreactivity in AD

- modifies clinicopathologic and radiologic phenotype. *Neurology* **70**, 1850-1857.
- [8] McKhann G, Drachman D, Folstein M, Katzman R, Price D, Stadlan EM (1984) Clinical diagnosis of Alzheimer's disease: Report of the NINCDS-ADRDA Work Group under the auspices of the Department of Health and Human Services Task Force on Alzheimer's disease. *Neurology* **34**, 939-944.
- [9] Crane PK, Carle A, Gibbons LE, Insel P, Mackin RS, Gross A, Jones RN, Mukherjee S, Curtis SM, Harvey D, Weiner M, Mungas D, Alzheimer's Disease Neuroimaging Initiative (2012) Development and assessment of a composite score for memory in the Alzheimer's Disease Neuroimaging Initiative (ADNI). *Brain Imaging Behav* **6**, 502-516.
- [10] Franklin EE, Perrin RJ, Vincent B, Baxter M, Morris JC, Cairns NJ, Alzheimer's Disease Neuroimaging Initiative (2015) Brain collection, standardized neuropathologic assessment, and comorbidity in Alzheimer's Disease Neuroimaging Initiative 2 participants. *Alzheimers Dement* **11**, 815-822.
- [11] Montine TJ, Phelps CH, Beach TG, Bigio EH, Cairns NJ, Dickson DW, Duyckaerts C, Frosch MP, Masliah E, Mirra SS, Nelson PT, Schneider JA, Thal DR, Trojanowski JQ, Vinters HV, Hyman BT, National Institute on Aging; Alzheimer's Association (2012) National Institute on Aging-Alzheimer's Association guidelines for the neuropathologic assessment of Alzheimer's disease: A practical approach. *Acta Neuropathol* **123**, 1-11.
- [12] Grothe M, Heinsen H, Teipel S (2013) Longitudinal measures of cholinergic forebrain atrophy in the transition from healthy aging to Alzheimer's disease. *Neurobiol Aging* **34**, 1210-1220.
- [13] Grothe MJ, Barthel H, Sepulcre J, Dyrba M, Sabri O, Teipel SJ, Alzheimer's Disease Neuroimaging Initiative (2017) *In vivo* staging of regional amyloid deposition. *Neurology* **89**, 2031-2038.
- [14] Müller-Gärtner HW, Links JM, Prince JL, Bryan RN, McVeigh E, Leal JP, Davatzikos C, Frost JJ (1992) Measurement of radiotracer concentration in brain gray matter using positron emission tomography: MRI-based correction for partial volume effects. *J Cereb Blood Flow Metab* **12**, 571-583.
- [15] Gonzalez-Escamilla G, Lange C, Teipel S, Buchert R, Grothe MJ, Alzheimer's Disease Neuroimaging Initiative (2017) PETPVE12: An SPM toolbox for partial volume effects correction in brain PET - Application to amyloid imaging with AV45-PET. *Neuroimage* **147**, 669-677.
- [16] Desikan RS, Segonne F, Fischl B, Quinn BT, Dickerson BC, Blacker D, Buckner RL, Dale AM, Maguire RP, Hyman BT, Albert MS, Killiany RJ (2006) An automated labeling system for subdividing the human cerebral cortex on MRI scans into gyral based regions of interest. *Neuroimage* **31**, 968-980.
- [17] Teipel S, Heinsen H, Amaro E, Jr., Grinberg LT, Krause B, Grothe M, Alzheimer's Disease Neuroimaging Initiative (2014) Cholinergic basal forebrain atrophy predicts amyloid burden in Alzheimer's disease. *Neurobiol Aging* **35**, 482-491.
- [18] Goodman S (2008) A dirty dozen: Twelve P-value misconceptions. *Semin Hematol* **45**, 135-140.
- [19] Wagenmakers EJ, Marsman M, Jamil T, Ly A, Verhagen J, Love J, Selker R, Gronau QF, Smira M, Epskamp S, Matzke D, Rouder JN, Morey RD (2018) Bayesian inference for psychology. Part I: Theoretical advantages and practical ramifications. *Psychon Bull Rev* **25**, 35-57.
- [20] Kruschke JK (2015) *Doing Bayesian Data Analysis - A Tutorial with R, JAGS, and Stan*. Elsevier, San Diego, CA.
- [21] Teipel S, Temp AGM, Levin F, Dyrba M, Grothe MJ (2020) Association of PET-based stages of amyloid deposition with neuropathological markers of A β pathology. *Ann Clin Transl Neurol*, doi: 10.1002/acn3.51238
- [22] Scheinin NM, Gardberg M, Roytta M, Rinne JO (2018) Negative 11C-PIB PET predicts lack of Alzheimer's disease pathology in postmortem examination. *J Alzheimers Dis* **63**, 79-85.
- [23] Cerami C, Dodich A, Iannaccone S, Magnani G, Santangelo R, Presotto L, Marcone A, Gianolli L, Cappa SF, Perani D (2018) A biomarker study in long-lasting amnesic mild cognitive impairment. *Alzheimers Res Ther* **10**, 42.
- [24] Sabbagh MN, Schauble B, Anand K, Richards D, Murayama S, Akatsu H, Takao M, Rowe CC, Masters CL, Barthel H, Gertz HJ, Peters O, Rasgon N, Jovalekic A, Sabri O, Schulz-Schaeffer WJ, Seibyl J (2017) Histopathology and Florbetaben PET in patients incorrectly diagnosed with Alzheimer's disease. *J Alzheimers Dis* **56**, 441-446.
- [25] Rahayel S, Bocti C, Seigny Dupont P, Joannette M, Lavalée MM, Nikelski J, Chertkow H, Joubert S (2019) Subcortical amyloid load is associated with shape and volume in cognitively normal individuals. *Hum Brain Mapp* **40**, 3951-3965.